



Experimental Study on the Variation of Structural Strength of Undisturbed Loess

Zhihang Shi*, Deren Liu

Lanzhou Jiaotong University, Lanzhou, 730070, China

* 1205818525@qq.com

Abstract. This paper separately studies the friction strength and cementation strength of loess skeleton. The carbonate, silt and coarse particles serving as the skeleton structure in loess are separated, and carbonate samples, silt samples and skeleton particle samples are made. Then, direct shear tests are conducted on the samples. The variation laws of loess structure strength, friction strength and cementation strength with moisture content and vertical pressure are studied, and the degree of influence of friction strength and cementation strength on loess structure strength is explored. The results show that the structure strength, friction strength and cementation strength of loess all decrease with the increase of moisture content; with the increase of moisture content and vertical pressure, the proportion of carbonate and silt cementation strength in the structure strength of loess gradually decreases, while the proportion of friction strength in the structure strength of loess gradually increases.

Keywords: loess; structural strength; moisture content; vertical pressure

1 Introduction

The loess has obvious columnar joints and large pore structure. This special structural feature directly affects the mechanical properties and engineering characteristics of loess, and studying the structural strength variation characteristics of loess has certain theoretical value and practical significance in engineering. Xie Dingyi^[1] proposed an index that can reflect the structural characteristics of loess regarding the arrangement of particles and the influence of particle connection, and verified the rationality of this quantitative index through experiments. N. Phien-wej^[2] mainly studied the collapse and strength characteristics of Thai loess, and the research results indicated that the loose structure was the main reason for its easy collapse, and this structure was mainly attributed to the clay bridge bonds. Dang Jinqian^[3] analyzed the composition of the strength of unsaturated loess and the source of structural strength through direct shear tests, proposed a method for determining structural strength, and explored the relationship between loess structural strength and shear strength. Jozef Horabik^[4] measured the strength of artificial aggregates containing different proportions of kaolinite (as a binder) and feldspar (as a skeleton particle) through uniaxial compression tests. Tian Kanliang^[5] proposed that the structural strength of loess is composed of the chemical

bonding strength between soil particles and the friction strength between soil particles. However, the substances that can provide bonding strength are mainly carbonate salts and clay minerals. Therefore, this paper separated the clay minerals, carbonate salts, and coarse particles as the skeleton structure in loess, prepared clay mineral-cemented samples, carbonate-cemented samples, and skeleton particle samples, and conducted direct shear tests on all samples to analyze the characteristics of loess structural strength, friction strength, and bonding strength, and explore the strength of the influence degree of friction strength and bonding strength on loess structural strength.

2 Test Materials and Methods

2.1 Source of Test Soil Sample and its Basic Physical Properties

The test soil samples were collected from the northern mountain of Lanzhou City, Gansu Province. They are of light yellow homogeneous structure with pinhole-like pores. The samples were taken by the artificial chisel method and then wrapped tightly with cling film to prevent damage to the samples during transportation. The sampling process is shown in Figure 1. Physical and mechanical parameters tests were conducted on the undisturbed loess samples. The natural moisture content was 8%, the dry density was 1.59g/cm^3 , the liquid limit and plastic limit were 28% and 16% respectively, the plasticity index was 12%, and the specific gravity of soil particles was 2.7.



(a) Sampling location.



(b) Soil Clod Truncation.



(c) Sampling.



(d) Packaging soil samples.

Fig. 1. Sampling process of undisturbed loess.

2.2 Sample Preparation

Five sample types were prepared: intact loess, saturated remolded loess, skeleton particles, clay, and carbonate. Water contents were set at 8, 10, 12, 15, 17, and 20% for intact loess; 8, 10, 12, and 15% for other three types. All samples had a dry density of 1.59 g/cm³. Sample quantities were 24, 4, 16, 16, and 16 for each type respectively. Samples of undisturbed loess and saturated remolded loess were prepared according to the sampling methods specified in "Standard for geotechnical testing method" (GB/T 50123-2019).

The principle for preparing skeleton particle samples is that the mass ratio of quartz and feldspar in the sample should be consistent with that in the original state of loess; the particle size range should be the same as that of sand particles in the original state of loess. The particle size range of the sample can be obtained from Table 1, and the mineral composition and content of the sample can be known from Table 2 based on the mineral composition analysis of the original state of loess. Therefore, in the skeletal particle specimen, soil particles within the 0.075-0.25 mm size range account for 58.86% of the total mass. Within this specific particle size fraction, quartz sand constitutes 75.4% with a mass of 50.57 g, potassium feldspar occupies 15.3% with a mass of 10.25 g, and albite comprises 9.2% with a mass of 6.24 g. Subsequently, soil particles within the 0.25-0.5 mm size range represent 22.24% of the total specimen mass. In this particle size interval, quartz sand maintains a consistent proportion of 75.4% with a mass of 10.33 g, potassium feldspar retains 15.3% with a mass of 2.09 g, and albite persists at 9.2% with a mass of 1.28 g. Finally, soil particles within the 0.5-1 mm size range constitute 19.29% of the total specimen mass. Within this coarsest fraction, quartz sand continues to dominate at 75.4% with a mass of 11.27 g, potassium feldspar remains at 15.3% with a mass of 2.28 g, and albite sustains its 9.2% proportion with a mass of 1.39 g. The skeletal particle specimen can be systematically prepared by precisely combining these soil particle categories according to their specified size fractions and corresponding mass proportions as delineated above.

Table 1. Composition of intact loess particles.

1-0.25mm	0.25-0.075mm	0.075-0.005mm	<0.005mm
11.7%	13%	55.87%	18.43%

Table 2. Analysis of mineral composition of undisturbed loess.

Mineral	Percent	Mineral	Percent
Silicon Oxide	45.4%	Muscovite	8.5%
synthetic	14.7%	Albite	5.6%
Keokuk	11.5%	illite	3.3%
Benson Mines	9.2%	chlorite	1.8%

The clay particles in the clay sample were prepared by water method. The sifted air-dried soil was first soaked, boiled, cooled, and 4% sodium hemphetaphosphate solution was added, then the suspension was poured into the settling cylinder, and finally the suspension was fully stirred to make the soil particles settle in the water. Then, the

settling time t of soil particles $d > 0.005\text{mm}$ is calculated by equation (1). When the test reaches the time t , soil particles $d > 0.005\text{mm}$ will settle and accumulate at the bottom of the cylinder, while soil particles $d < 0.005\text{mm}$ float in the suspension. The test process is shown in Figure 2.

$$td^2 = K^2L_t \quad (1)$$

Where: t is the settling time of soil particles with $d > 0.005\text{ m}$; s ; d is the diameter of soil particles, mm; K is the calculation coefficient of soil particle size, which is obtained according to the " Standard for geotechnical testing method " (GB/T50123-2019); L_t is the fall distance of soil particles in water in t time, cm.

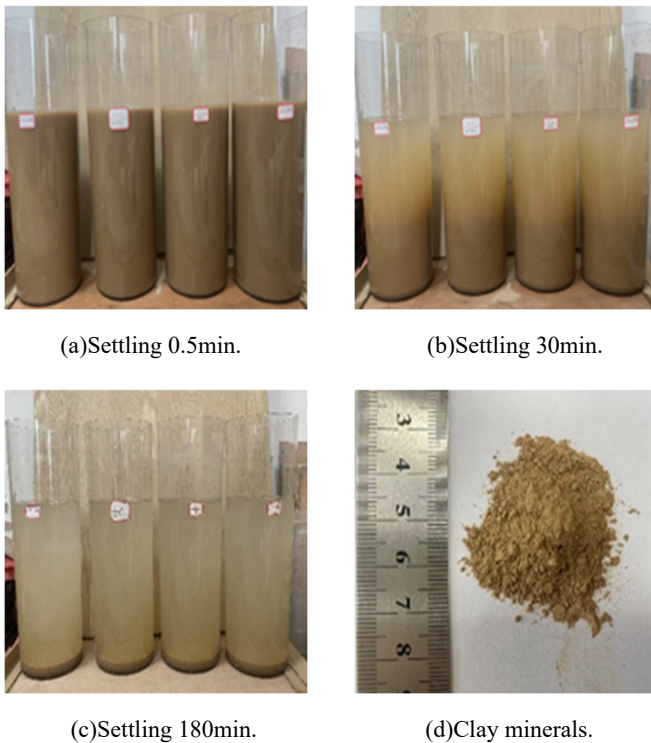
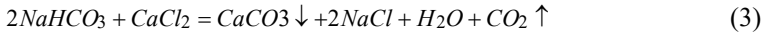
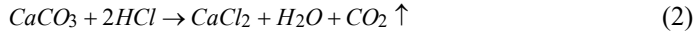


Fig. 2. Moisture method test process.

In this test, the sedimentation distance L_t was 34 cm, and the suspension was sucked out by siphon principle after standing for 180 min, and the clay particles were separated by filtration^[6]. Combine 14.37g of clay with 81.47gThe clay sample with 15% clay content was prepared by mixing the skeleton particles evenly.

It can be seen from Table 2 that the main salt substance in loess is calcium carbonate. Therefore, 14.37g carbonate powder ($d=0.045\text{mm}$) and 81.47g skeleton particles are mixed evenly to make a carbonate sample with 15% calcium carbonate content. Considering that the direct mixing of calcium carbonate powder and skeleton particles in

the sample preparation method could not give full play to the cementation effect of calcium carbonate in the sample, a chemical reaction method was adopted to add chemical reagents to precipitate calcium carbonate in the sample to strengthen the skeleton particles^[7], and the chemical reaction equations were shown in equations (2) and (3).



Drop the corresponding mass of concentrated hydrochloric acid into the sample. Calcium carbonate powder will undergo a chemical reaction with the concentrated hydrochloric acid to produce calcium chloride. Then, add sodium bicarbonate solution. It will react with calcium chloride, and the generated carbonate ions combine with calcium ions to form gelatinous crystals. These gelatinous crystals are mainly distributed in the particle pores and between particles, playing the role of filling and cementation. The test process is shown in Figure 3.



(a) hydrochloric acid.



(b) sodium bicarbonate.



(c) Drop in reagent.



(d) Dry out.

Fig. 3. Calcium carbonate curing process.

2.3 Test Methods

The direct shear test is conducted by applying horizontal loads to cause shear deformation in the specimens until the structure fails. Usually, four sets of specimens are selected for the test, which are loaded under normal stress conditions with gradient variations. The shear displacement and peak shear strength at the time of specimen failure are recorded, and then the shear strength index of the soil is calculated using Coulomb's law. In this test, the ZJ-type strain-controlled direct shear apparatus is used, with the shear rate controlled at 0.8 mm/min. The vertical pressures applied are 100, 200, 300, and 400 kPa. For the loess specimens, the peak strength or the shear stress at the shear displacement of 4 mm on the shear stress-shear displacement curve under the above vertical pressures is taken as the shear strength. The shear stress-shear displacement curves of loess specimens with different moisture contents under different vertical pressures are tested respectively.



Fig. 4. ZJ strain controlled direct shear instrument.

3 Study on Structural Strength Characteristics Of Loess

3.1 Definition of Structural Strength of Loess

Figure 5 shows: Curve 1 - intact loess stress-strain curve; Curve 2 - saturated remolded loess curve; Curve 3 - deviatoric stress difference (termed loess structural strength curve) between curves 1 and 2. q_o and q_s represent intact and saturated remolded loess strengths (τ) at strain ε . Saturated remolded loess exhibits disrupted particle arrangement, destroyed cementation, and weakened frictional structure due to saturation^[8]. Structural strength equals $q_o - q_s$ at identical ε .

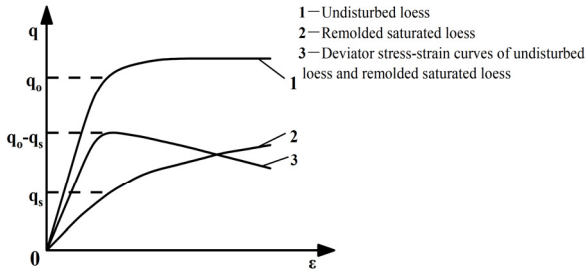
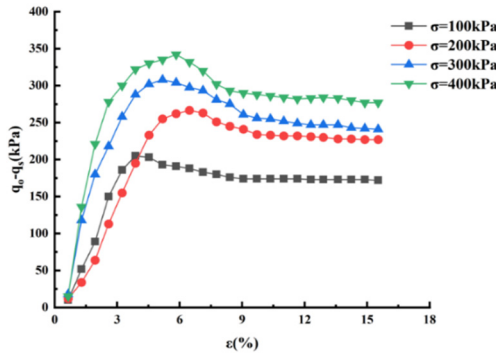


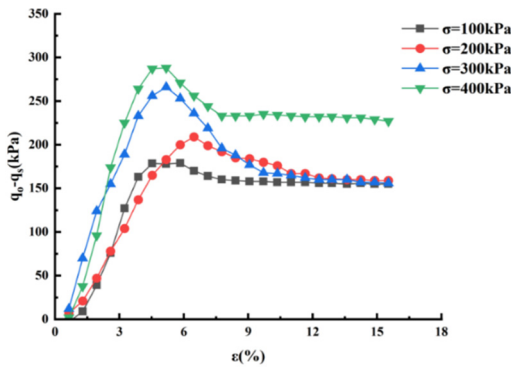
Fig. 5. Stress-strain curves of undisturbed loess and saturated remolded loess.

3.2 Strength Development Curve of Loess Structure

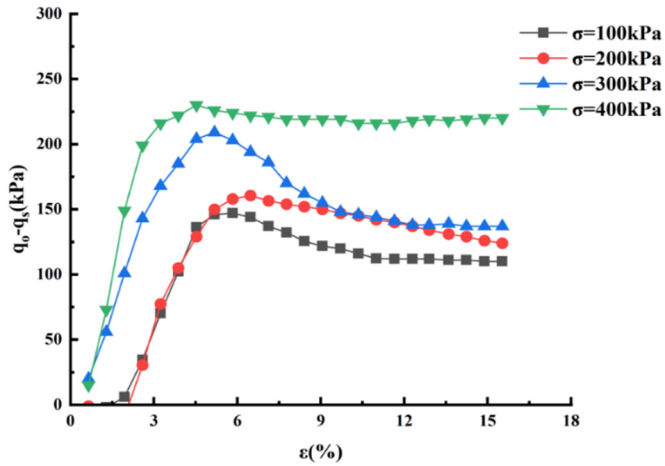
According to the method for obtaining the strength of loess structure in Figure 5, the curves showing the variation of the strength of loess structure with the increase of strain under different moisture contents are plotted in Figure 6, so as to facilitate the analysis of the relationship between the original strength of loess structure and the moisture content.



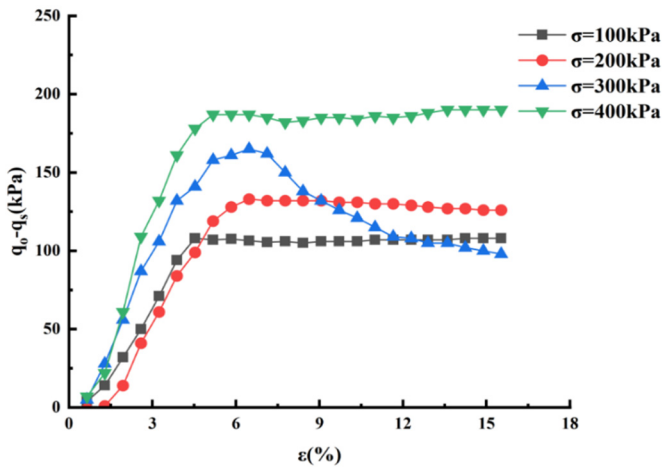
(a) $w=8\%$



(b) $w=10\%$



(c) $w=12\%$



(d) $w=15\%$

Fig. 6. The curves representing the development of the original state of soil's structural strength under different moisture contents.

As can be seen from Figure 6, the abscissa represents strain ε and the ordinate represents the original soil structure strength $q_o - q_s$. For each water content and vertical pressure, there is a peak point on the soil structure strength curve, which is located within the strain range of 4-7%. This peak is what we commonly refer to as the strength of the soil body when it is destroyed, that is, the maximum structural strength value that the soil body can withstand. The original soil structure strength gradually decreases with the increase of water content. At a vertical pressure $\sigma = 400$ kPa, the maximum structural strength of the soil body is as high as 342 kPa. As the water content increases,

the maximum structural strength decreases to a minimum of 87 kPa. The original soil structure strength gradually increases with the increase of vertical pressure. For example, at a water content $w = 10\%$, although the structural strength curves under different vertical pressure conditions intersect, the maximum structural strength increases with the increase of vertical pressure. At a vertical pressure $\sigma = 100$ kPa, the maximum structural strength is 179 kPa, and at a vertical pressure $\sigma = 400$ kPa, the maximum structural strength is 288 kPa. Through the above analysis, it can be known that the maximum structural strength of the soil body is affected by the factors of water content and vertical pressure. The variation curve of the original soil structure strength can be divided into two stages. In the first stage, within the strain range of 0-7%, the original soil structure strength increases sharply with the increase of strain, and the soil structure strength is fully exerted. In the second stage, within the strain range of 7-15%, the original soil structure strength either decreases rapidly to remain unchanged with the increase of strain or decreases slowly to remain unchanged with the increase of strain, indicating that the soil structure is in the adjacent failure stage when the maximum structural strength value is reached, and the soil particles have a relative sliding tendency. After the maximum structural strength value, the soil particles slide, and the original structure of the soil is destroyed. As the strain gradually increases, the soil particles are arranged and connected with each other to form secondary structures, and the external force cannot destroy the secondary structures, thus the variation curve of the structural strength is in a gentle state.

3.3 Analysis of Influencing Factors of Structural Strength of Loess

It can be inferred from Figure 7 that under various vertical load conditions, the structural strength ($q_o - q_s$) of undisturbed loess exhibits a continuous attenuation characteristic as the moisture content (w) increases. When the moisture content of the soil mass is below the threshold value of 14%, the decline rate of the structural strength is relatively rapid. Once the moisture content surpasses this threshold, the attenuation trend significantly slows down.

This non-linear variation pattern is in good agreement with the moisture-sensitivity characteristic of the mechanical properties of loess. In a low-moisture state, the loess shows a relatively high sensitivity to moisture. This is because the internal structure of the loess at low moisture content is more susceptible to the influence of water molecules. The addition of a small amount of water can disrupt the original particle-to-particle bonding forces, leading to a rapid reduction in the structural strength.

Conversely, under high-moisture conditions, the sensitivity of the loess to moisture weakens. At this stage, most of the pores in the loess are already filled with water, and the water has already played a major role in softening the structure. Further increasing the moisture content has a relatively small impact on the overall mechanical properties. This characteristic is specifically reflected in the curve of the structural strength versus moisture content, where the slope of the curve gradually decreases from a large value to a small value, indicating the change in the sensitivity of the structural strength to the moisture content.

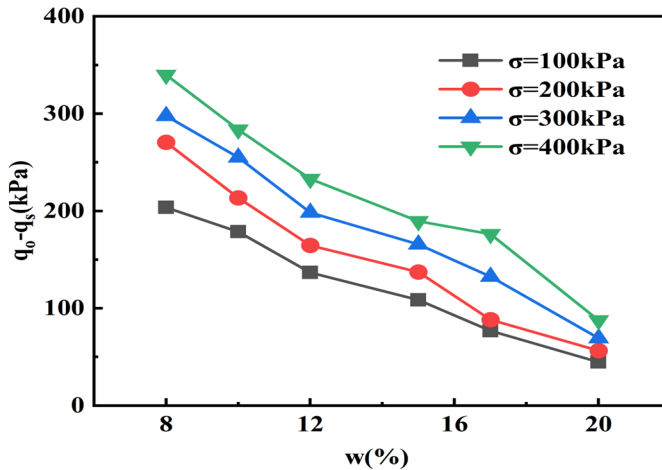


Fig. 7. Relationship between loess structural strength and moisture content.

3.4 Research on Friction Strength Characteristics of Loess

To better explore the characteristics of the frictional strength of soil particles in undisturbed loess, direct shear tests were conducted on skeleton particle samples. The relationship between the frictional strength of skeleton particles and moisture content is plotted in Figure 8.

As shown in the figure, at the same moisture content, the frictional strength ($\sigma \tan \varphi$) of skeleton particles increases with the vertical pressure (σ). The four curves span a wide band, indicating that the vertical pressure significantly affects the frictional strength.

At a constant vertical pressure, the frictional strength decreases with increasing moisture content. When $\sigma = 400$ kPa, $\sigma \tan \varphi$ shows a rapid decline. The smaller the σ , the slower and smaller the decrease in $\sigma \tan \varphi$. This suggests that the frictional strength is influenced by both moisture content and vertical pressure.

This indicates that the frictional strength is also affected by the moisture content. This is due to the lubrication effect of water and the action of matric suction. As the moisture content increases, the lubrication effect of water is fully exerted, reducing the frictional force when soil particles move out of position relative to each other. Meanwhile, the matric suction formed by capillary tension gradually decreases as the moisture content rises, thereby weakening the frictional strength^[9].

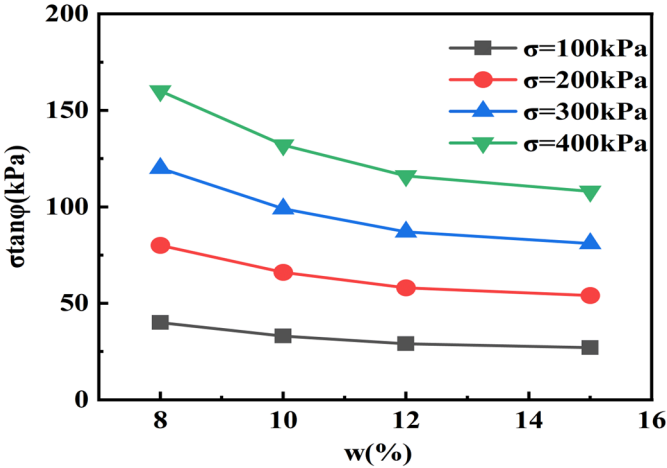


Fig. 8. Relationship between granular skeleton frictional strength and moisture content.

3.5 Study on Cementation Strength Characteristics of Loess

As shown in Figure 9, both clay-cementation strength (C_n) and carbonate-cementation strength (C_i) decrease with increasing moisture content (w). At $w = 8\%$, mean C_i and C_n reached 80.35 kPa, declining to 36.8 kPa at $w = 15\%$, indicating significant moisture dependence. C_i slightly exceeded C_n at identical w . Within $w = 8\text{--}15\%$, C_i decreased by 7.06 kPa per 1% w increase, versus 4.37 kPa for C_n , demonstrating stronger moisture sensitivity for carbonate cementation.

The reduction in clay-cementation strength (C_n) with increasing moisture content is attributed to thickened hydration films on particle surfaces, which reduce direct interparticle contacts and weaken bonding forces^[10]. Similarly, carbonate-cementation strength (C_i) decline stems from cementation degradation: (1) partial dissolution of carbonates in water induces cement loss; (2) intergranular spacing increases due to water molecule intercalation, diluting cementation materials, collectively reducing C_i with moisture rise^[11].

4 Proportional Contribution Analysis of Frictional and Cementation Strengths in Loess Structural Strength

Figure 10 presents the percentages of clay particle strength ($C_n/(q_o - q_s)$), carbonate cementation strength ($C_i/(q_o - q_s)$), and skeletal particle frictional strength ($\sigma \tan \phi / (q_o - q_s)$) within the structural strength of undisturbed loess under varying moisture contents and vertical pressures. Under identical vertical pressure, both $C_n/(q_o - q_s)$ and $C_i/(q_o - q_s)$ progressively decrease with increasing moisture content, whereas $\sigma \tan \phi / (q_o - q_s)$ exhibits a gradual enhancement. At constant moisture content, $\sigma \tan \phi / (q_o - q_s)$ increases with ascending vertical pressure, reaching 57% under high vertical pressure ($\sigma = 400$ kPa) and declining to a minimum of 20% under low vertical pressure ($\sigma = 100$ kPa).

Conversely, $C_n/(q_o - q_s)$ and $C_t/(q_o - q_s)$ demonstrate progressive reduction with elevated vertical pressure.

For moisture contents ($w = 8\%, 10\%, 12\%$, and 15%) and vertical pressures ($\sigma = 100, 200, 300,$ and 400 kPa), the averaged values reveal the following trends: $C_n/(q_o - q_s)$ registers $28.25\%, 27.5\%, 26.5\%$, and 24.5% respectively; $C_t/(q_o - q_s)$ measures $33\%, 30\%, 29.75\%$, and 26.5% correspondingly; while $\sigma \tan\phi/(q_o - q_s)$ displays progressive increments of $34.5\%, 34\%, 38.25\%$, and 42.5% across the moisture content spectrum.

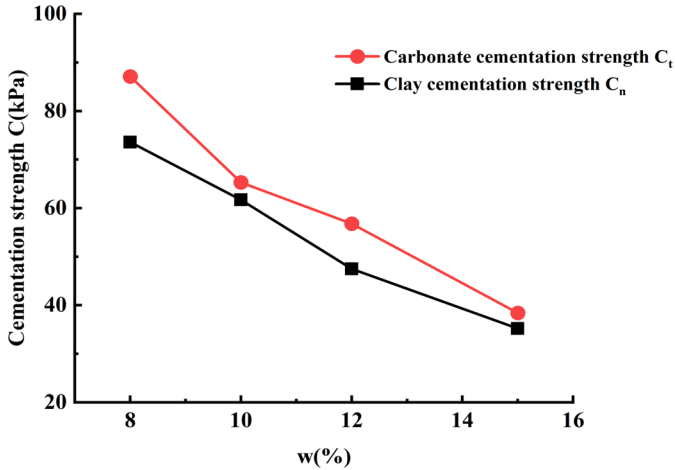


Fig. 9. Clay- and carbonate-cementation strengths versus moisture content.

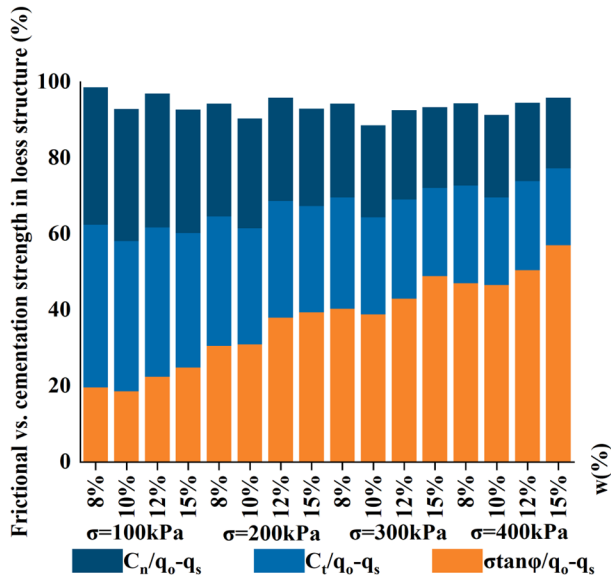


Fig. 10. The percentage contributions of cementation strength and frictional strength to the structural strength of loess.

5 Conclusions and Prospects

5.1 Conclusion

(1) Loess structural strength ($q_o - q_s$) reflects post-destruction weakening magnitude. Saturated remolded soil exhibits destroyed cementation and friction weakening via saturation. q_o subtracts q_s at identical strain ε defines intact loess structural strength.

(2) The original loess exhibits unique structural evolution characteristics during the shear process, and its stress-strain curve presents a typical two-stage response pattern. Experimental data show that when the shear strain reaches the critical value, the mechanical response of the sample undergoes a fundamental transformation. Before the critical shear strain, as the shear action continues to intensify, the shear stress shows a significant positive growth trend. This stage corresponds to the stage where the original structure of the soil maintains its integrity, and the intrinsic cementation effect and particle arrangement characteristics of the soil can be fully demonstrated. After the shear action exceeds the critical threshold, the shear stress response shows a progressive weakening feature. At this time, micro-structural reorganization occurs within the soil: the original particle cementation system begins to disintegrate, and a new contact network gradually forms. This structural reconfiguration process directly leads to the non-linear attenuation characteristics of the mechanical response.

(3) The structural strength of loess is primarily influenced by moisture content and vertical pressure. As the moisture content decreases and vertical pressure increases, the structural strength of undisturbed loess increases. At a constant vertical pressure, the structural strength of undisturbed loess decreases with increasing moisture content. With constant moisture content, the structural strength increases as vertical pressure rises. The larger the vertical pressure, the greater the decrease in structural strength. At lower moisture content, the structural strength of undisturbed loess is more sensitive to changes in vertical pressure, whereas at higher moisture content, the structural strength shows less variation with changes in vertical pressure.

(4) As moisture content decreases, the clay cementation strength (C_n), carbonate cementation strength (C_t), and friction strength ($\sigma \tan \phi$) increase. C_n and C_t are more sensitive to moisture content, with C_n slightly lower than C_t at the same moisture content. $\sigma \tan \phi$ is primarily influenced by vertical pressure.

(5) As moisture content decreases, the ratios of $C_n/(q_o - q_s)$ and $C_t/(q_o - q_s)$ increase, while $\sigma \tan \phi/(q_o - q_s)$ decreases. With higher vertical pressure, the ratios of $C_n/(q_o - q_s)$ and $C_t/(q_o - q_s)$ decrease, while $\sigma \tan \phi/(q_o - q_s)$ increases. The clay cementation strength ($C_n/(q_o - q_s)$) accounts for approximately 27%, carbonate cementation strength ($C_t/(q_o - q_s)$) for 30%, and skeletal particle friction strength ($\sigma \tan \phi/(q_o - q_s)$) for 37% of the total structural strength of loess.

5.2 Prospects

The study of loess structural strength remains a prominent research focus. Although this work conducted extensive experimental investigations on loess structural strength, frictional strength, and cementation strength, revealing specific variation patterns,

current understanding still faces theoretical gaps and technical bottlenecks due to constraints in research cycles, experimental conditions, cognitive limitations, and the absence of robust engineering validation mechanisms. Building on existing findings, future research should: (1) Perform comparative experiments on vertical profiles at varying depths to establish depth-gradient models of structural strength, while advancing regional variability studies through parallel experiments on representative loess profiles in typical distribution areas to construct strength evolution maps incorporating regional differentiation. (2) In the future, it is necessary to conduct comparative analysis on the formation mechanisms, humidity sensitivity and engineering applicability differences of the structural strength of loess and the viscosity strength of polymers, in order to optimize the soil improvement techniques.

References

1. Xie, D., and Qi, J., "Soil structure characteristics and new approach in research on its quantitative parameter," *Chinese Journal of Geotechnical Engineering*,1999,(06):651-656,doi:[10.11779/CJGE199906001](https://doi.org/10.11779/CJGE199906001).
2. Phien-wej,N., Pientong,T., and Balasubramaniam,A,S., "Collapse and strength characteristics of loess in Thailand," *Engineering Geology*,1992,32,(1-2):59-72,doi:[10.1016/0013-7952\(92\)90018-t](https://doi.org/10.1016/0013-7952(92)90018-t).
3. Dang, J., and Li, J., "The relationship characteristics between the shear strength of unsaturated loess and its structural strength," *Yangtze River*,2001,38,(01):79-83+90,doi:[10.13243/j.cnki.slxh.2001.07.014](https://doi.org/10.13243/j.cnki.slxh.2001.07.014).
4. Horabik,J., and Jozefaciuk,G., "Structure and strength of kaolinite–soil silt aggregates: Measurements and modeling," *Geoderma*,2021,382,doi:[10.1016/j.geoderma.2020.114684](https://doi.org/10.1016/j.geoderma.2020.114684).
5. Tian,K., Zhang,H., and Ma,J., "Test study of loess structure based on static strength conditions," *Rock and Soil Mechanics*,1999,33,(07):1993-1999,doi:[10.16285/j.rsm.2012.07.004](https://doi.org/10.16285/j.rsm.2012.07.004).
6. Liu,B., Zhou,H., and Yang,B., "Experimental research on the influence of clay content and water content ratio on the strength characteristics of red clay," *Water Resources and Hydro-power Engineering*,2024,55,(07):147-156,doi: [10.13928/j.cnki.wrahe.2024.07.013](https://doi.org/10.13928/j.cnki.wrahe.2024.07.013).
7. Zhang,X.,Ye,W., and Liu,Z., "Advances in soil cementation by biologically induced calcium carbonate precipitation," *Rock and Soil Mechanics*,2022,43,(02):345-357,doi: [10.16285/j.rsm.2021.1249](https://doi.org/10.16285/j.rsm.2021.1249).
8. Tian,K., and Zhang,H., "EXPERIMENTAL STUDY OF LOESS STRUCTURAL PROPERTIES BASED ON SOIL DEFORMATION," *Chinese Journal of Rock Mechanics and Engineering*,2010,29,(08):1706-1712.
9. Xiao,J.,Yan,W., and Qiao,S., "Experimental research on the influence of dry density and moisture content on the shear strength of standard sand, " *Journal of Railway Science and Engineering*,2023,20,(10):3789-3797,doi:[10.19713/j.cnki.43-1423/u.t20230768](https://doi.org/10.19713/j.cnki.43-1423/u.t20230768).
10. Bao,L., and Wei,F., "Macroscopic and microscopic analysis of the effects of moisture content and dry density on the strength of loess," *Science Progress*,2024,107,(03):1-17,doi: [10.1177/00368504241261592](https://doi.org/10.1177/00368504241261592).
11. Wang,H.,Ni,W.,Yuan,K., and Ren,S., "An experimental study on the behavior of loess-clay mixtures upon wetting and its implications for tillage on the Loess Plateau," *Soil and Tillage Research*,2024,240,1-12,doi:[10.1016/j.still.2024.106071](https://doi.org/10.1016/j.still.2024.106071).

Open Access This chapter is licensed under the terms of the Creative Commons Attribution-NonCommercial 4.0 International License (<http://creativecommons.org/licenses/by-nc/4.0/>), which permits any noncommercial use, sharing, adaptation, distribution and reproduction in any medium or format, as long as you give appropriate credit to the original author(s) and the source, provide a link to the Creative Commons license and indicate if changes were made.

The images or other third party material in this chapter are included in the chapter's Creative Commons license, unless indicated otherwise in a credit line to the material. If material is not included in the chapter's Creative Commons license and your intended use is not permitted by statutory regulation or exceeds the permitted use, you will need to obtain permission directly from the copyright holder.

